A COMBINATION OF NORMALIZED DIFFERENCE VEGETATION INDEX AND MULTI-TEMPORAL RADAR VEGETATION INDEX OF SENTINEL DATA FOR LANDUSE/LANDCOVER CLASSIFICATION

Le Minh Hang[1], Nguyen Dinh Duong[2] and Tran Anh Tuan[3]

[1]Le Quy Don Technical University, 236 Hoang Quoc Viet Street, Bac Tu Liem District, Hanoi, Vietnam
Email: leminhhang81@lqdtu.edu.vn
[2]Institute of Geography, Vietnam Academy of Science and Technology, 18 Hoang Quoc Viet Street, Cau Giay District, Hanoi, Vietnam,
Email: duong.nguyen2007@gmail.com
[3]Institute of Ecology and Biological Resources, Vietnam Academy of Science and Technology, 18 Hoang Quoc Viet Street, Cau Giay District, Hanoi, Vietnam
Email: tuan.ig@gmail.com

KEY WORDS: LULC, NDVI index, RVI index, Sentinel images

ABSTRACT: Landuse/Landcover (LULC) plays an essential role in managing and monitoring natural resources and the environment in many countries. Optical satellite imagery provides a primary data source for LULC mapping. Unfortunately, the application of the optical image is limited due to the effects of clouds, especially in the tropical area in Vietnam. Microwave imagery can observe during the day and night with nearly all-weather capability. Currently, Sentinel-1 satellite with microwave sensor, operated by the European Space Agency, supplies SAR data with global coverage free of charge. This article presents the combination of the Normalized Difference Vegetation Index (NDVI) of Sentinel-2 data and the multi-temporal Radar Vegetation Index (RVI) of Sentinel-1 data for LULC mapping. The Support Vector Machine (SVM) method was used and the classification accuracy achieved 86%. The study area is in Hanoi, Vietnam, with many landcover features and various plants such as fruit trees, paddy rice. As a result, combining the NDVI index and the multi-temporal RVI index can classify the species of trees and help to improve the applicability of Sentinel satellite data in landcover change monitoring.

1. INTRODUCTION

LULC data is an essential input data in monitoring earth surface, such as human and natural effects and prediction of changes. Human activities are rapidly changing the LULC, especially in urban which the cropland is changed to built-up land or barren land.

Earth observation has obtained many achievements in recent years thanks to modern Earth observation satellite systems with sizeable remote sensing data sources, which were used as a tool for LULC mapping (Clerici, 2017; Huong, 2020; Ienco, 2019; Khan, 2020). Sentinel satellites are part of the Copernicus program developed by the European Space Agency (ESA). Sentinel-1 and Sentinel-2 satellites are some of the satellites of the Copernicus program that provide satellite images for observation of the Earth's surface. Sentinel-1 satellite carries a dual-polarized microwave sensor with C band. Sentinel-2 satellite carries an optical sensor. The two Sentinel satellites data are providing with a high revisit time and free of charge. With Landsat satellite, Sentinel satellite data will be a high-resolution remote sensing data source for effective natural resource monitoring.

Optical satellite images are currently the primary data in studies on LULC mapping, in which landcover is mainly classified based on the spectral reflectance characteristics of the objects. However, optical imagery has the disadvantage of being influenced by clouds, especially in tropical monsoon areas like Vietnam. Meanwhile, microwave satellite has acquired data during day and night, not affected by clouds. However, LULC classification by using microwave imagery needs expert knowledge because of the noise signal and backscatter characteristics on the image. Many studies have proposed the combination of the optical image and SAR (Synthetic Aperture Radar) images for LULC mapping. The common method used the combination data, which include the multi-spectral band of the optical image and the multi-temporal SAR bands to classify LULC (Steinhausen, 2018). The accuracy of these method is over 85% (Hischmugl, 2018; Steinhausen, 2018; Ienco, 2019; Khan 2020). The second method used the combination of texture indices of SAR image and the vegetation indices of the optical image to map LULC (Barret, 2016). (Clerici, 2017) uses texture parameters in the GLCM matrix of Sentinel-1 image and NDVI (Normalized Difference Vegetation Index), S2REP (Sentinel-2 Red Edge Position index), GNDVI (Green Normalized Difference Vegetation Index), MSAVI (Modified Soil Adjusted Vegetation Index) of Sentinel-2 image to classify LULC with 88.75% accuracy. Using index on images Sentinel-1 and Sentinel-2 has been proposed in other studies (Chatziantoniou, 2017; Ienco, 2019; Tavares, 2019; Nguyen, 2020).

RVI (Radar Vegetation Index) index, which is one of the indexes of SAR polarized data, has been studied and proven to correspond to the vegetation growth (Kim, 2012; Bousbih, 2017; Mandal, 2020) and correlate with the NDVI index of optical images (Kim, 2014; Gonenc, 2019). Many studies have suggested combining RVI and NDVI index to

monitor different plant densities (Agapiou, 2020), soil moisture and crops land (Szigarski, 2018; Mandal, 2020), plant growth (Rath, 2020). Hence the RVI index on the SAR polarized image proved to reflect the change of the Earth's surface, especially for plant objects.
In this article, the authors proposed to combine the NDVI index of the Sentinel-2 image and the multi-temporal RVI index of the Sentinel-1 image for LULC mapping, case study in Hanoi, Vietnam.

2. STUDY AREA AND MATERIALS

2.1. Study area

The Ha Noi is located in the Viet Nam's Red River delta, with an average elevation of 5m to 20m above sea level, in which some hilly areas are north, northwest and south of Hanoi, with elevation from 20m to over 400m. The topography of Ha Noi decreases height from north to south and from west to east. The topographic form is the high alluvial terraces interspersed with lakes. The Hanoi climate is hot in the summer, rainy and cold winter, less rainy. With tropical location zone, Hanoi areas get much solar radiation and high temperatures around the year. The total radiation averages 11,8 kcal/cm2, and the year average temperature is 23,6°C. Hanoi temperature is relatively high in humidity and rainfall due to the influence of the East Sea. The average annual humidity is around 79% a year, and rainfall is 1,800 mm. Approximately 114 days are raining a year here.
The location of study area is in the suburbs and the southwest of Hanoi (Figure 1). The study area has various land cover objects, including built-up land with urban and rural area, cultivated land, cropland, fruit tree land, water land.

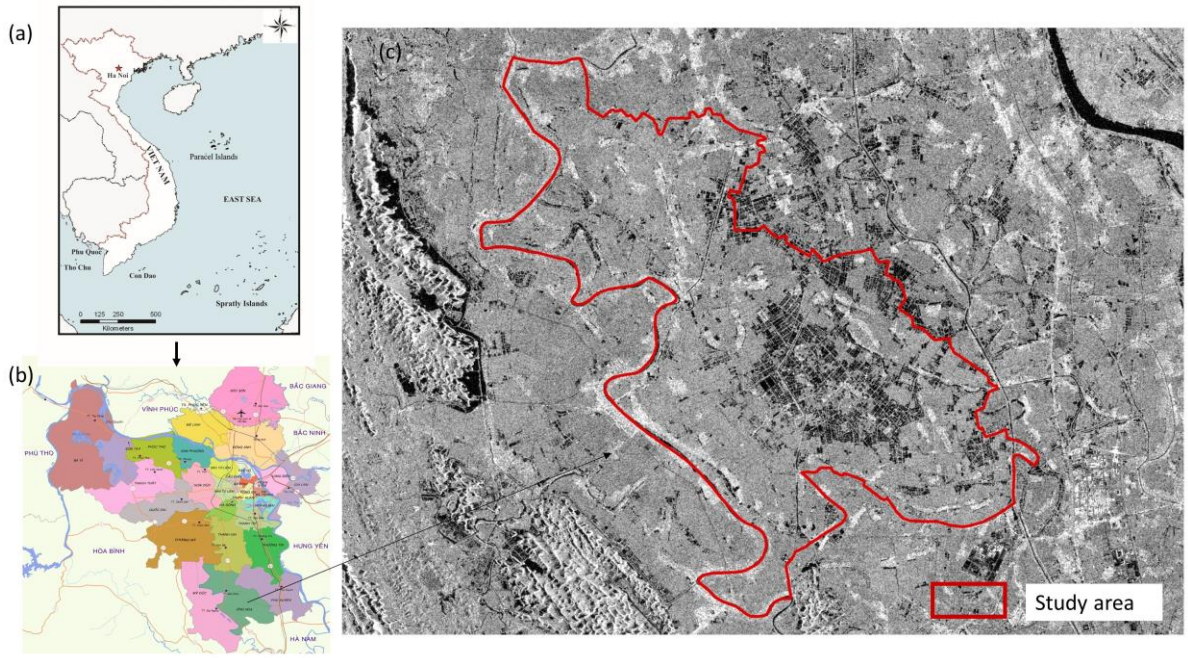

Figure 1. The location of the study area. (a) Location Hanoi in Vietnam; (b) Administrative map of Hanoi; (c) VH polarization of Sentinel-1

2.2. Materials

The materials included Sentinel-2 images and multi-temporal Sentinel-1 images. The characteristics of these materials are shown in Table 1. Sentinel-2 data was collected from May 2019 to November 2019 because this is the time of winter crop in the Red River Delta. Meanwhile, Sentinel-1 data was collected from May 2019 to April 2020, with one image per month used to evaluate land cover change in one year.

Table 1. The characteristic of the materials

	Sentinel-2	Sentinel-1
Acquisition time	19/05/20219, 28/06/2019, 07/08/2021, 06/09/2019, 21/09/2019, 01/10/2019, 05/11/2019, 10/11/2019,25/11/2019	30/05/2019, 23/06/2019, 17/7/2019, 10/8/2019, 27/9/2019, 10/08/2019, 17/9/2019, 9/10/2019, 14/11/2019, 20/12/2019, 25/01/2020, 18/02/2020, 25/03/2020, 30/4/2020
Data product	BOA (surface reflectance)	Interferometric Wide (IW) – GRDH
Polarization		VV-polarization and VH-polarization
Imaging frequency	Blue; Green; Red; NIR; SWIR-1; SWIR-2	C-band (5.46 Hz)
Resolution	10m	10m
Bit depth	16 bit	16 bit

Firstly, Sentinel-2 data was collected and pre-processed using Google Earth Engine (GEE) platform, including the following steps: (1) Convert data to BOA (Bottom of Atmosphere) reflectance; (2) Cloud removing; (3) Subset data by the boundary of the study area.Sentinel-2 The Sentinel-2 data was selected from May 2019 to May 2020 with cloud coverage percent below 10% in the cloud removing algorithm and the cloud objects were detected using QA60 band.

Secondly, the multi-temporal Sentinel-1 data was pre-processed by using SNAP Toolbox software which includes the main steps such as (1) Remove Thermal noise; (2) Calibration (convert to sigma nought); (3) Terrain correction (using SRTM 1sec); (4) Convert linear to dB; (5) Subset data by the boundary of the study area. The pre-processing was performed with VV polarization and VH polarization band.

3. METHODOLOGY

3.1. The vegetation index of Sentinel-2 and Sentinel-1 images

NDVI is a standard vegetation index for measuring surface reflectance and giving a quantitative estimation of plants growth. The NDVI index is a vegetation index commonly used to study plants and land cover mapping by using optical images (Bousbih, 2017; Clerici, 2017; Agapiou, 2020). The data used to calculate NDVI is Sentinel-2 cloudless, and the signal value is the surface reflectance value. The NDVI is a ratio of the difference between near-infrared (NIR) and red (RED) reflectance divided by their sum as follow:

$$NDVI = \frac{NIR - RED}{NIR + RED} \quad (2)$$

Where: NIR -Near-infrared band, corresponding to band 8 of Sentinel-2 data; RED - Red band, corresponding to band 8 of Sentinel-2 data.

NDVI observes the health of plants and a measure of photosynthetic activity within the range -1 to 1. Low NDVI values indicate a little vegetation cover, and higher values indicate a higher green vegetation density. The NDVI values near zero and negative values indicate non-vegetated features, such as barren surfaces, water (Figure 2b).

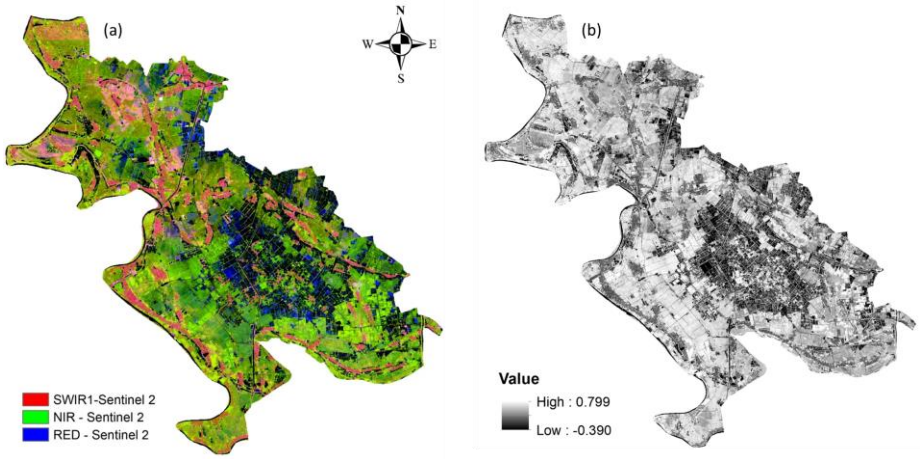

Figure 2. (a) RGB composite of Sentinel-2; (b) NDVI image

RVI is one of the established active microwave indices for mapping vegetation density (Arii, 2010). In particular, some studies have compared RVI to optical-based measures like the NDVI. (Szigarski, 2019) showed that RVI isolated the scattering by vegetation and was independent of soil surface reflectivity, moisture, and roughness. The RVI index was proposed by (Kim and van Zyl 2004, 2009) and applied to full polarized images with VV, VH, HH and HV polarization. However, (Charbonneau, 2005) assumed $\sigma_{HH} \approx \sigma_{VV}$ and proposed the equation for calculating RVI with the dual-polarization data as follows:

$$RVI = \frac{4\sigma_{VH}}{\sigma_{VV} + \sigma_{VH}} \quad (3)$$

Where: σ_{VV} - Sigma nought value of VV polarization; σ_{VH} - Sigma nought value of VH polarization;

However, the unit of the polarization coefficient in Equation (3) is the power unit. Therefore, the parameters of Equation (3) are converted from dB to power unit by Equation (4):

$$RVI = \frac{10^{4|\sigma_{VH}dB|/10}}{10^{|\sigma_{VV}dB|/10} + 10^{|\sigma_{VH}dB|/10}} \quad (4)$$

Sentinel-1 data currently has dual-polarization data with VV and VH polarization, so the RVI index is computed by Eq.4. The RVI index of the Sentinel-1 materials from August 2019 to April 2020 (Table 1).

Figure 3 shows the multi-temporal RVI values of the landcover features. We analyse multi-temporal RVI values of two different elements: vegetation features (Paddy rice, Fruit tree) and non-vegetation features (Barren land, Built-up, Water). For non-vegetative parts, RVI values are usually low, less than 1.5, and stable in the period. In contrast, RVI values of vegetation features are higher and changes in response to plant growth. For example, the RVI value of paddy rice features changes in August, September, October, and November, corresponding to the growth cycle of paddy rice in the winter crop. The fruit tree features have a high RVI value and are relatively stable in the period. Hence, we propose to use multi-temporal RVI values for the classification of landcover features in this article.

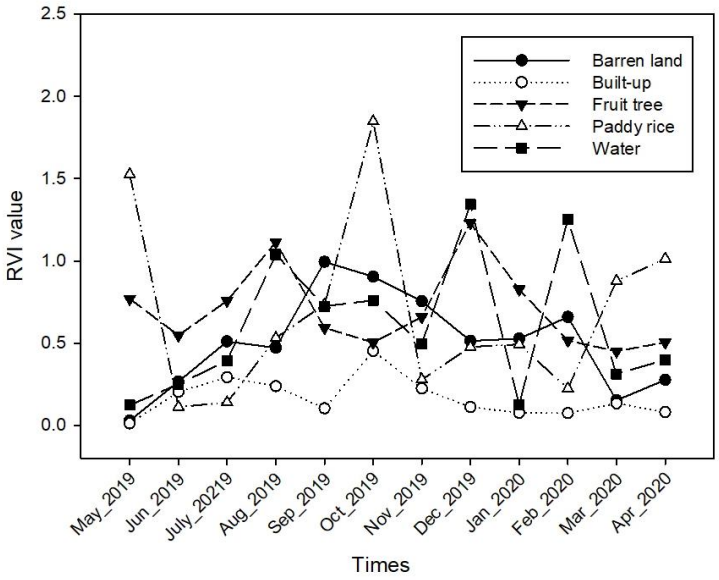

Figure 3. Multi-temporal RVI value of landcover features

3.2. Proposed method

The proposed method is shown in Figure 4 and consists of four main steps:

- Sentinel-2 and Sentinel-1 are pre-processed using the GEE platform and SNAP Toolbox software
- Calculating NDVI and multi-temporal RVI indices.
- Creating a combination indices image with NDVI+(max, min, average, standard deviation of RVI images)
- Classifying the combination indices image by the SVM method.

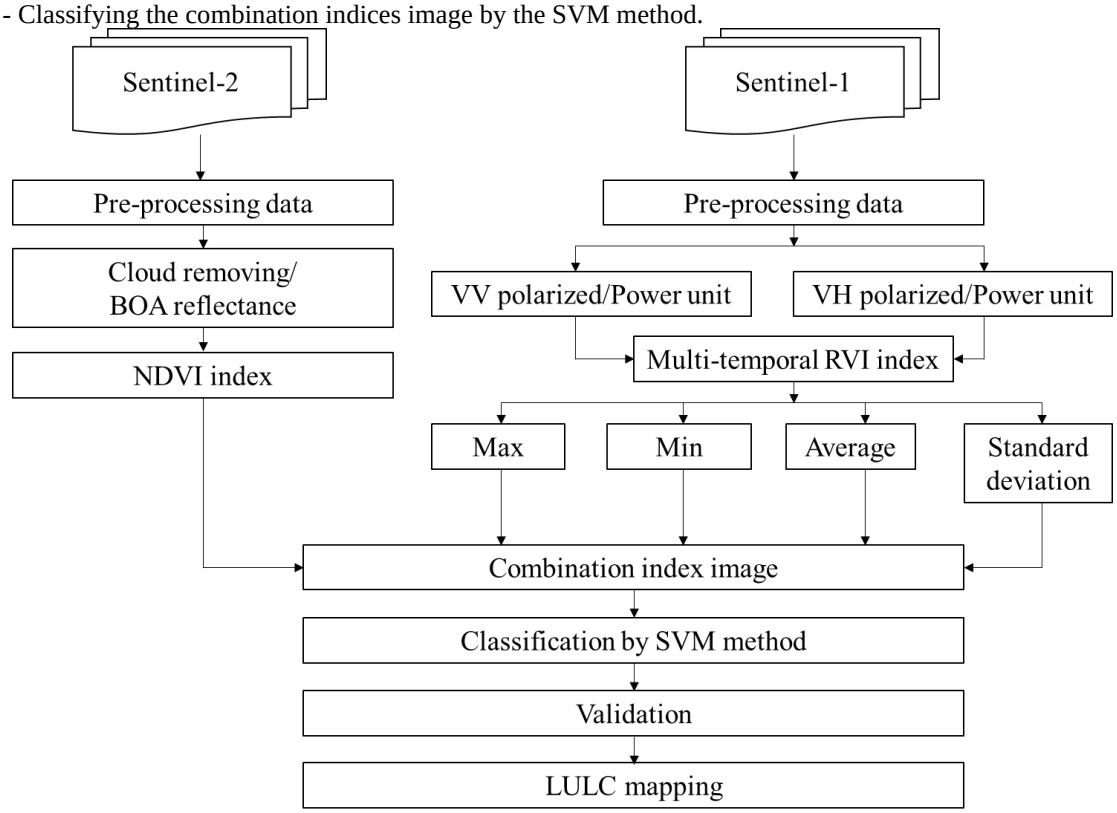

Figure 4. The flowchart of the proposed method

In the second step, the NDVI index image was calculated based on the cloudless image data from May 2019 to November 2019 (Figure 2b), which is the time of winter crop. Comparing NDVI images (Figure 2b) and RGB colour composite images (Figure 2a) is to be interpreted into three main objects: plants (high NDVI), barren land, built-up (medium NDVI) and water (low NDVI).

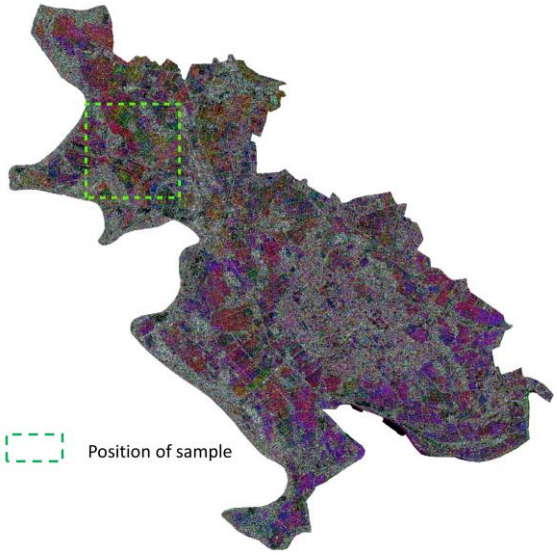

Figure 5. RGB composite of multi-temporal RVI (R:G:B = 7/2019:6/2019:5/2019)

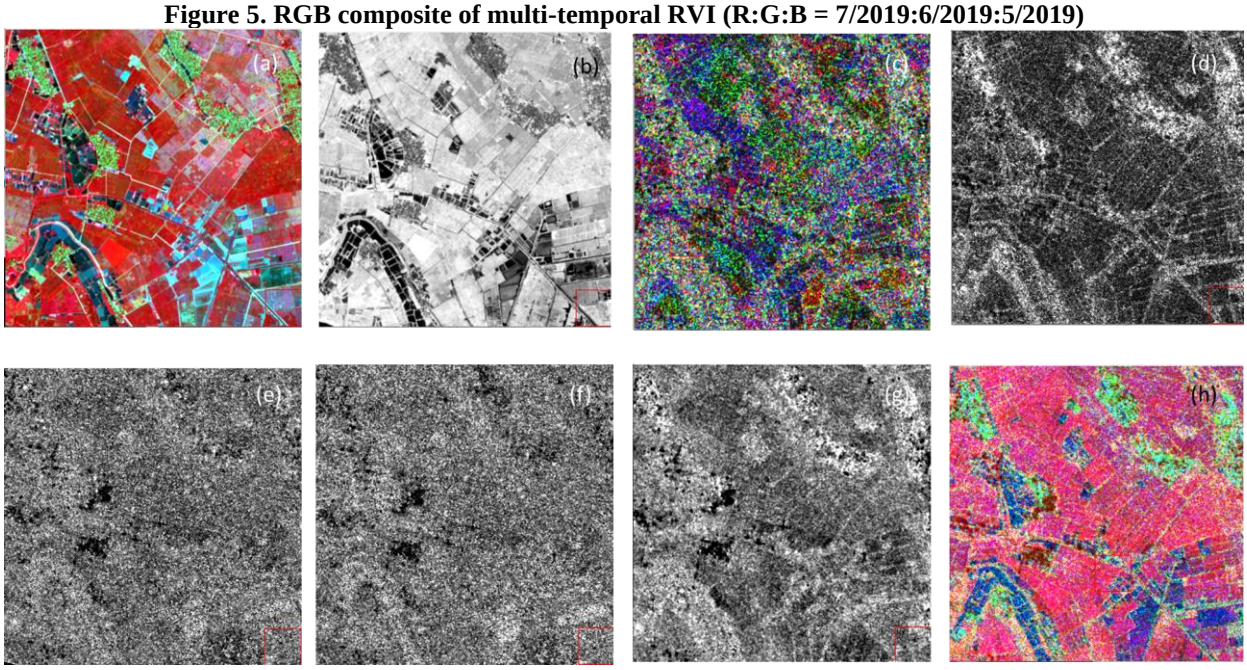

Figure 6. Comparision of index images. (a) RGB composite of Sentinel-2 (NIR:Red:Green); (b) NDVI image of Sentinel-2; (c) RGB composite of multi-temporal RVI (Jul/2019:Jun/2019:May/2019); (d) Max RVI index; (e) Min RVI index; (f) Average RVI index; (g) Standard deviation RVI index; (h) RGB composite of the combination indexes image (R:G:B = NDVI:Min:Max)

Figure 5 shows the RGB colour composite image of the multi-temporal RVI image. To analyze and compare the index images of Sentinel-2 and RVI images, we selected a sample region with the location is shown in Figure 5. Figure 6c shows an RGB colour composite image of multi-temporal RVI data. Comparison between Figure 6a and Figure 6c shows that landcover features have a different colour in the RGB composite image of multi-temporal RVI data. Base on the analysis of Figure 3 and Figure 6, the authors proposed to calculate index images including max (Figure 6d), min (Figure 6e), average (Figure 6f), and standard deviation (Figure 6g). Figure 6h is an RGB composite indexes image corresponding to NDVI:Max: Min band. The colours of (Figure 6h) allow us to interpret landcover features, including barren land, built-up, water, paddy rice, and fruit tree.

4. Results and discussion

The combination indexes image is the input data for landcover classification using SVM method. The ROI samples are integrated based on the RGB composite of Sentinel-2 (Figure 2a) and the RGB composite of the combination indexes (Figure 6h). The results are shown in Figure 7 with five classes: water, paddy rice, fruit tree, built-up, and

barren land. Table 2 shows the confusion matrix for assessing the classification accuracy in which the overall accuracy was 86% with a kappa index of 0.8122. According to table 2, the classification accuracy of water objects is the highest with 97.59%. The lowest accuracy is the fruit tree object, which is confused with the paddy rice object because of the same as the plant. Besides, paddy rice and fruit tree features have the same spectral reflectance properties on optical images. However, the RVI value changed corresponding to the growth of paddy rice, while it was stable for the fruit tree features (Figure 3). Therefore, paddy rice and fruit tree features have different values on combination indexes classified by the SVM algorithm. The classification accuracy of paddy rice is 84.8%, and that of fruit trees is 81.7%.

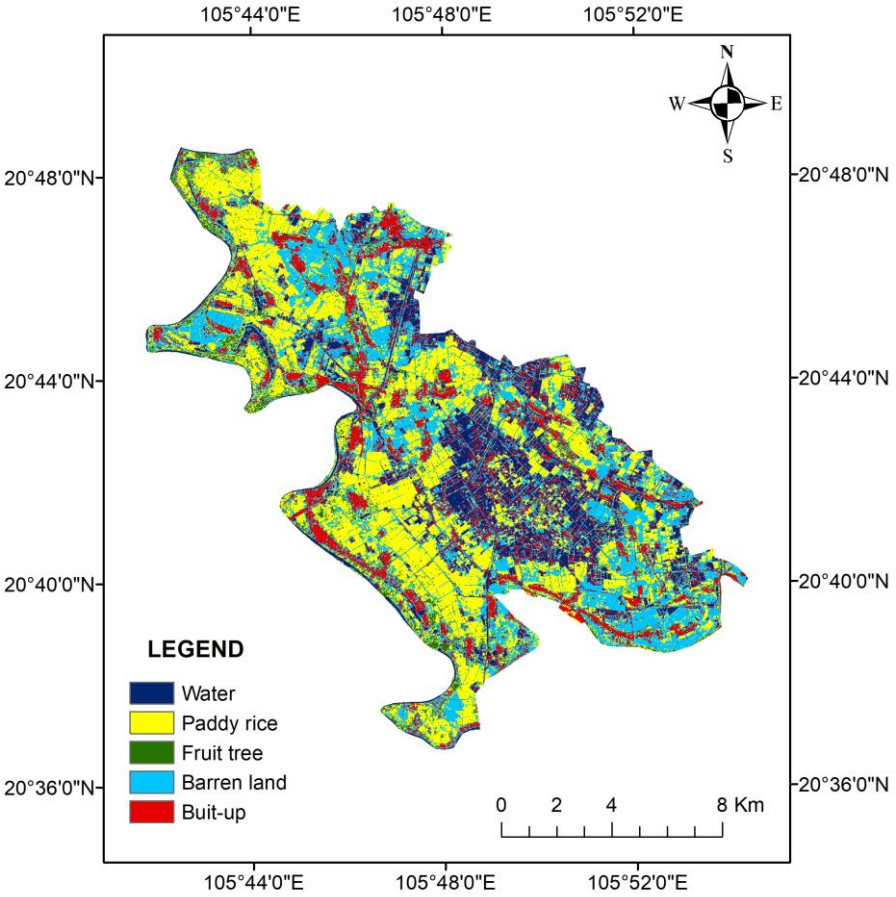

Figure 7. Land cover mapping by using the combination indexes image

Table 2. Assessment of classification accuracy

	Water	Paddy rice	Fruit tree	Barren land	Built-up	Total pixel	UA (%)
Water	608	0	0	3	12	623	**97.6**
Paddy rice	0	2012	185	158	19	2374	**84.8**
Fruit tree	0	118	541	2	1	662	**81.7**
Barren land	1	157	3	1501	131	1793	**83.7**
Built-up	39	0	1	74	871	985	**88.4**
Total	648	2287	730	1738	1034	6437	
PA (%)	**93.8**	**88.0**	**74.1**	**86.4**	**84.2**		
	Overall accuracy = 86%						
	Kappa index = 0.8122						

5. Conclusion

In conclusion, the Sentinel-1 and Sentinel-2 data are proved to apply landcover mapping with a high resolution of 10m. The multi-temporal RVI index calculated by the VV and VH polarization images of the Sentinel-1 data correlates with plants' growth and changes by time. The multi-temporal RVI can classify non-vegetation or vegetation features, significantly discriminate with paddy rice and fruit tree. However, the RGB colour composite image of the

multi-temporal RVI images has much speckle noise. Hence, the authors proposed combining the multi-temporal RVI of Sentinel-1 data with the NDVI image of Sentinel-2 data with a spatial resolution of 10m. The composite indexes image includes NDVI, max, min, average, and standard deviation images. The classification accuracy of the combined index image achieved 86% with the Kappa index of 0.8122, in which the accuracy of the water feature is the highest with 97.6%. The fruit tree object has the lowest classification accuracy with 81.7% and is often confused with the paddy rice feature. In the future, we will study multi-temporal RVI of different plant species to determine the correlation between the RVI index with field measurements and the species' growth.

References

Agapiou, A., 2020. Estimating Proportion of Vegetation Cover at the Vicinity of Archaeological Sites Using Sentinel-1 and -2 Data, Supplemented by Crowdsourced OpenStreetMap Geodata. Applied sciences, 10 (4764), pp. 2-17.

Arii, M., van Zyl, J. J., Kim, Y., 2010. A General Characterization for Polarimetric Scattering From Vegetation Canopies. IEEE TRANSACTIONS ON GEOSCIENCE AND REMOTE SENSING, 48(9), pp. 3349-3357.

Barrett, B., Raab, C., Cawkwell, F., Green, S., 2016. Upland vegetation mapping using Random Forests with optical and radar satellite data. Remote Sensing in Ecology and Conservation, pp. 212-231.

Bousbih, S., Zribi, M., Zohra, L-C., Baghdadi, N., Hajj, M. E., Gao, Q., Mougenot, B., 2017. Potential of Sentinel-1 Radar Data for the Assessment of Soil and Cereal Cover Parameters. Sensors, 17(2617), pp. 1-19.

Chatziantoniou, A., Petropoulos, G. P., Psomiadis, E., 2017. Co-Orbital Sentinel-1 and 2 for LULC Mapping with Emphasis on Wetlands in a Mediterranean Setting Based on Machine Learning. Remote sensing, 9(1259), pp. 1-19.

Charbonneau, F., Trudel, M., Fernandes, R., 2005. Use of Dual Polarization and MultiIncidence SAR for soil permeability mapping. In: Advanced Synthetic Aperture Radar (ASAR) 2005, St-Hubert, Canada.

Clerici, N., Calderon, C. A. V., Posada, J. M., 2017. Potential of Sentinel-1 Radar Data for the Assessment of Soil and Cereal Cover Parameters. Journal of Maps, 13(2), pp. 718-726.

Gonenc, A., Ozerdem, M. S., Acar, E., 2019. Comparison of NDVI and RVI Vegetation Indices Using Satellite Images. 2019 8th International Conference on Agro-Geoinformatics (Agro-Geoinformatics) , pp. 1-4.

Hischmugl, M., Sobe, C., Deutscher, J., Schardt, M., 2018. Combined Use of Optical and Synthetic Aperture Radar Data for REDD+ Applications in Malawi. Land, 7(116), pp. 1-20.

Huong, T. T. N., Trung, M. D., Erkki, T. Ronald, E. M., 2020. Land Use/Land Cover Mapping Using Multitemporal Sentinel-2 Imagery and Four Classification Methods—A Case Study from Dak Nong, Vietnam. Remote sensing, 12(1367), pp. 1-27.

Ienco, D., Interdonato, R., Gaetano, R., Minh, D. H. T., 2019. Combining Sentinel-1 and Sentinel-2 Satellite Image Time Series for land cover mapping via a multi-source deep learning architecture. ISPRS Journal of Photogrammetry and Remote Sensing, 158 (2019), pp. 11–22.

Kim, Y., van Zyl, J, 2004. Vegetation effects on soil moisture estimation. Geoscience and Remote Sensing Symposium. In Proceedings of the IEEE International 2004, IGARSS ’04, Anchorage, AK, USA, 20–24 September 2004; Volume 2, pp. 800–802.

Kim, Y.J., VanZyl, J., 2009. A time-series approach to estimate soil moisture using polarimetric radar data. IEEE Trans. Geosci. Remote Sens. Vol. 47, 2519–2527.

Kim, Y., Jackson, T., Lee, H., Hong, S., 2012. Radar Vegetation Index for Estimating the Vegetation Water Content of Rice and Soybean. IEEE GEOSCIENCE AND REMOTE SENSING LETTERS, 9(4), pp. 1-5.

Kim, Y. H., Oh, J. H., Kim, Y. I., 2014. Comparative Analysis of the Multispectral Vegetation Indices and the Radar Vegetation Index. Journal of the Korean Society of Surveying, Geodesy, Photogrammetry and Cartography, 32(6), pp. 607-615.

Khan, a., Govil, H., Kumar, G., Dave, R., 2020. Synergistic use of Sentinel-1 and Sentinel-2 for improved LULC mapping with special reference to bad land class: a case study for Yamuna River floodplain, India. Spatial Information Research, 28, pp. 669-681.

Mandal, D., Ratha, D., Bhattacharya, A., Kumar, V., McNairn, H., Rao, Y. S., Frery, A. C., 2020. A Radar Vegetation Index for Crop Monitoring Using Compact Polarimetric SAR Data. IEEE TRANSACTIONS ON GEOSCIENCE AND REMOTE SENSING, 58(9), pp. 6321-6335.

Nguyen, T. T. H., Chau, T. N. Q., Pham, T. A., Tran, T. X. P., Phan, T. H., Pham, T. M. T., 2020. Mapping Land

use/land cover using a combination of Radar Sentinel -1A and Sentinel-2A optical images. OP Conf. Series: Earth and Environmental Science, 652(2021), pp. 1-12.

Qiu, J., Crow, W. T., Wagner, W., Zhao, T., 2019. Effect of vegetation index choice on soil moisture retrievals via the synergistic use of synthetic aperture radar and optical remote sensing. International Journal of Applied Earth Observation and Geoinformation, 80 (2019), pp. 47–57.

Ratha, D., Mandal, D., Dey, S., Bhattacharya, A., Frery, A., Rao. Y.S., McNairn, H., 2020. New vegetation indicies for full and compact polarimetric SAR data: In preparation for the Radarsat Constellation Mission (RCM). ISPRS Annals of the Photogrammetry, Remote Sensing and Spatial Information Sciences, Volume IV-3/W2-2020, pp. 1-6.

Steinhausen, M. J., Wagner, P. D., Narasimhan, B., Waske, B., 2018. Combining Sentinel-1 and Sentinel-2 data for improved land use and land cover mapping of monsoon regions. International Journal of Applied Earth Observation and Geoinformation, 73 (2018), pp. 595-604.

Szigarski, C., Jagdhuber, T., Baur, M., Thiel, C., Parrens, M., Wigneron, J. P., Entekhabi, D., 2018. Analysis of the Radar Vegetation Index and Potential Improvements. Remote sensing, 10(1776), pp. 1-15.

Tavares, P. A., Beltrao, N. E. S., Guimaraes, U. S., Teodoro, A. C., 2019. Integration of Sentinel-1 and Sentinel-2 for Classification and LULC Mapping in the Urban Area of Belém, Eastern Brazilian Amazon. Sensors, 19(1140), pp. 1-20.

Tran, A. T., Nguyen, K. A., Liou, Y. A., Le, M. H., Vu, V. T., Nguyen, D. D., 2021. Classification and Observed Seasonal Phenology of Broadleaf Deciduous Forests in a Tropical Region by Using Multitemporal Sentinel-1A and Landsat 8 Data. Forests, 12(235), pp. 1-19.